Photodiagnosis and Photodynamic Therapy 45 (2024) 103897

Contents lists available at ScienceDirect

Photodiagnosis and Photodynamic Therapy

journal homepage: www.elsevier.com/locate/pdpdt

Macrophages as a photosensitizer delivery system for photodynamic therapy: Potential for the local treatment of resected glioblastoma

Catherine Christie [a], Steen J Madsen [b], Qian Peng [c], Henry Hirschberg [a,b,*]

[a] Beckman Laser Institute, University of California, Irvine, CA 92617, USA
[b] Department of Health Physics & Diagnostic Sciences, University of Nevada, Las Vegas, NV 89154, USA
[c] Pathology Clinic, 4Department of Radiation Biology, Rikshospitalet-Radiumhospitalet HF Medical Center, University of Oslo, Oslo, Norway

ARTICLE INFO

Keywords:
Photodynamic therapy
Macrophage delivery
Blood brain barrier
Photosensitizer

ABSTRACT

Background: Photodynamic therapy (PDT) efficacy is determined in part by the concentration of photosensitizer (PS) at the treatment site. The blood-brain barrier (BBB) poses a significant limitation on the transport of PS into the post-operative resection region where brain tumors most often recur. Macrophages (Ma), as opposed to free or nanoparticle bound agents, are known to actively migrate to and around tumors, and can therefore be used as delivery vectors for both drugs and photosensitizers.
Methods: Mouse Ma (RAW264.7) and F98 rat glioma cells were used in all experiments along with the photosensitizer $AlPcS_{2a}$. Mitomycin-treated Ma were loaded with photosensitizer (PS) and mixed with glioma cells, forming hybrid spheroids. F98 spheroids were incubated with supernatants derived from PS-loaded Ma (Ma^{PS}). Light treatment (PDT) was administered at various radiant exposures from a 670 nm diode laser. The growth of both types of spheroids was evaluated by measurement of spheroid volume after 14 days in culture.
Results: PDT on F98 cell spheroid cultures, mediated by either free or PS-released from Ma, demonstrated a significant growth inhibition with supernatants harvested after 4 and 24 h. A significant PDT-induced growth inhibition was demonstrated in the Ma^{PS}/F98 hybrid spheroid experiments.
Conclusion: Since the efficacy of PDT, mediated by either free or released photosensitizer was comparable, the uptake and released photosensitizer was not degraded. Ma^{PS}, incorporated in hybrid tumor spheroids also mediated effective PDT. These results indicate that Ma have potential as an effective vector for photosensitizer delivery to resected brain tumors.

1. Introduction

Cytoreductive surgery is the primary modality in the treatment of glioblastoma. This is followed by post-operative radiation and chemo therapies. Despite these therapies, the tumors recur in close to 100 % of cases, with about 80 % of recurrences in the vicinity of the surgical resection cavity [1–3]. Therefore, an important aim of post-operative treatment is the sterilization of both the nests of tumor cells and the migrating glioma stem cells remaining at the margins of the resection cavity while minimizing damage to the surrounding brain tissue.

PDT has been tried in multiple clinical studies and extensively reviewed in recent publications [4–6]. As with many other forms of alternative therapies, results of clinical trials utilizing PDT for glioma therapy have been marginal. One feature of malignant gliomas that may account for the low efficacy of PDT in clinical trials is the limited concentration of photosensitizer (PS) at the target site caused by the BBB. Since the migratory and infiltrating glioma cells remaining in the resection cavity walls are protected by the BBB, the concentration of systemically or orally delivered photosensitizer is insufficient for effective PDT.

One method of bypassing the BBB is the use of circulating cells as delivery vectors. In particular, Ma offer several advantages compared to nanoparticles as targeted delivery vehicles. Ma are known to actively migrate to and infiltrate brain tumors [7–9]. They are drawn by chemotactic factors secreted by tumor cells and thereby migrate to tumors via an active process, obtaining access despite vascular and stromal barriers as well as the elevated interstitial pressure characteristic of most tumors. In previous studies, the feasibility of delivering loaded nanoparticles or water-soluble drugs to tumor cells using Ma was clearly demonstrated [10–17].

* Corresponding author at: Beckman Laser Institute, University of California, Irvine, CA 92617, USA.
E-mail address: hhirschb@uci.edu (H. Hirschberg).

https://doi.org/10.1016/j.pdpdt.2023.103897
Received 3 October 2023; Received in revised form 15 November 2023; Accepted 17 November 2023
Available online 19 November 2023

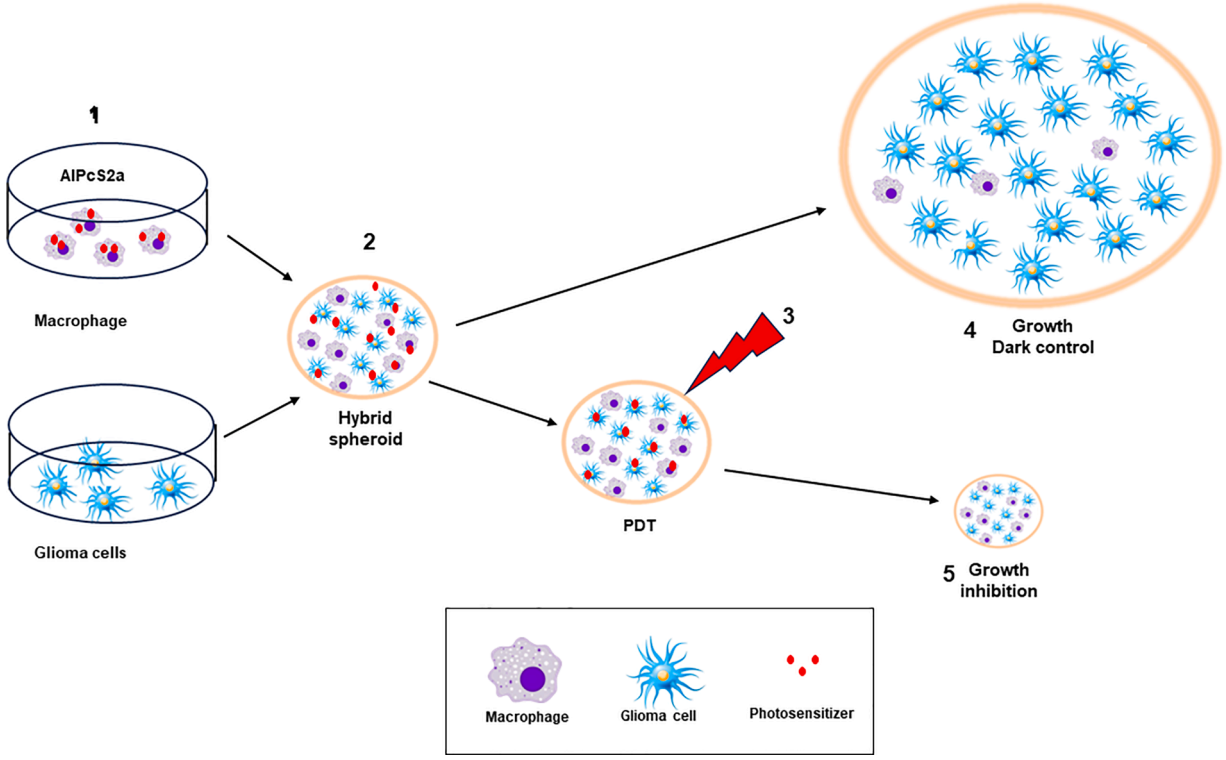

Fig. 1. Graphic of hybrid spheroid Ma^{PS} mediated PDT. (1) Ma incubated with photosensitizer (2) F98 glioma cells combined with Ma^{PS}, form hybrid spheroid. PS release. (3) PS taken up by glioma cells, light treatment (PDT). (4) Dark control, spheroid grows to 1 mm maximum size,. (5) PDT treated hybrid spheroid, growth inhibition/cessation.

The aim of the present *in vitro* research was designed to examine the ability of Ma to act as delivery vehicles for photosensitizers. Release characteristics of Ma loaded with the photosensitizer disulfonated aluminum phthalocyanine ($AlPcS_{2a}$) were evaluated for their ability to inhibit the growth of F98 monolayers and 3-D glioma spheroids following PDT. The basic experimental setup using F98/Ma hybrid spheroids is shown in Fig. 1.

2. Materials and methods

2.1. Cell lines and drug

Mouse macrophages (RAW264.7) and F98 rat glioma cells were obtained from the American Type Culture Collection (Manassas, VA). Both cell lines were maintained in Advanced DMEM medium (Life Technologies, Carlsbad, CA) supplemented with 2 % heat-inactivated fetal bovine serum (FBS), 25 mM HEPES buffer, 100 U/ml penicillin and 100 μg/ml streptomycin at 37 °C, 5 % CO_2 and 95 % humidity. The F98 and Ma were grown as monolayers in T 25 tissue culture flasks (Greiner BioOne, Frickenhausen, Germany) or in 9 cm flat-bottom square dishes (Simport Scientific Beloeil, Quebec, Canada).

2.2. Ma PS supernatant production

Ma were incubated in medium containing 2 μg/ml $AlPcS_{2a,}$ (Frontier Scientific, Inc., Logan, UT) for 4 h. The Ma were then incubated for 1 h with 20 μg/ml of mitomycin to prevent their proliferation. Ma were washed 4 times to remove all non-incorporated PS and the cultures were incubated in fresh medium. The Ma were then plated out into 5 wells in a 24-well plate (1 ml/well.) The supernatants (SN) were harvested from individual wells after 0.25, 2, 4, 24 and 48 h. Supernatants were also harvested from monolayers of "empty" Ma (not pulsed with PS) to act as controls.

2.3. Fluorescence microscopy of loaded Ma

Ma (3×10^4) were plated out in 35 mm glass bottom imaging dishes (Nunc, Thermo Fisher Scientific, USA). The dishes were incubated in culture medium for 24 h to allow the Ma to adhere. The medium was replaced with fresh medium containing 2 μg/ml of $AlPcS_{2a}$ for 4 h. The incubation was terminated by a double wash in clear buffer to remove non-incorporated $AlPcS_{2a}$. Fluorescence microscopy was performed after 1, 4 and 24 h in order to evaluate the time release of $AlPcS_{2a}$.

2.4. PDT using harvested supernatants on F98 monolayers

F98 monolayers were formed in the wells of 96-well flat bottom plates with 2.5×10^3 cells in 50 μl of culture medium per well (Corning Inc., NY). The plates were maintained at 37 °C in a 5 % CO_2 incubator for 24 h. Twenty-four hours after monolayer generation, 150 μl of the various collected SN, were added to the wells in fresh medium. Twenty-four hours after supernatant was added, light treatment, λ= 670 nm, from a diode laser (Intense; Cedar Knolls, NJ, USA) at an irradiance of 2.0 mW/cm^2 was administered for 10 min. corresponding to a radiant exposure of 1.2 J/cm^2. Determination of F98 cell growth and cell viability was carried out by the 3-(4,5-dimethylthiazol-2-yl)−5-(3-carboxymethoxyphenyl)−2-(4-sulfophenyl)−2H-tetrazolium, MTS assay (Promega, Madison, WI). Following PDT treatment, incubation was continued for 48 h at which point the culture medium was replaced with fresh clear buffer containing MTS reagents and incubated for a further 2 h. The optical density was read using an ELx800uv Universal Microplate Reader (Bio-Tek Instruments, Inc, Winooksi, WI).

2.5. PDT using harvested supernatants on F98 spheroids

F98 spheroids were formed by a modification of the centrifugation method previously described [18]. F98 glioma spheroids were generated with 2.5×10^3 cells in 20 μl of culture medium per well of an ultra-low

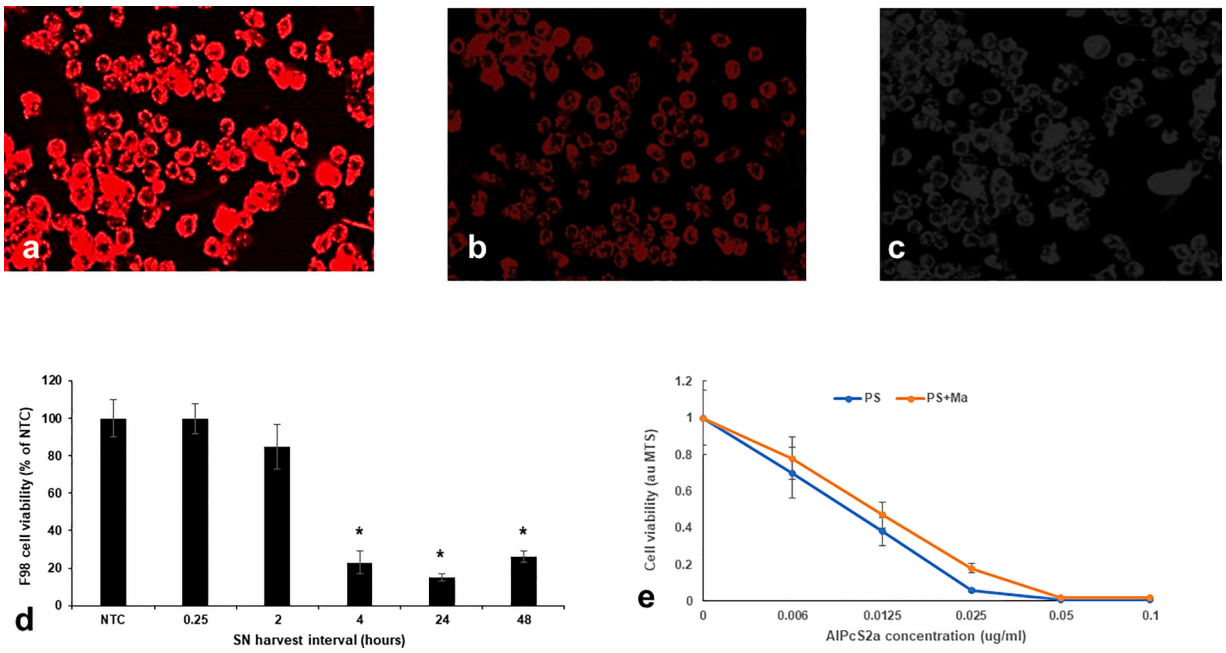

Fig. 2. (**a**) Fluorescence microscopy of AlPcS2a loaded Ma 1 h after loading. (**b**) 4 h after loading. (**c**) 24 h after loading. (**d**) Viability of F98 cell monolayers following SP released (SN) mediated PDT. SN harvested over a range, 0.25 to 48 h. Light treatment 1.2 J/cm^2. (**d**) AlPcS2a mediated PDT in the presence and absence of Ma. F98 2.5 K +/- Ma 2.5 K. Light treatment 1.2 J/cm^2. Cell viability assayed with MTS assay 48 h after PDT. Each data point represents the average cell viability of 6 monolayers. Error bars, standard deviation. * significant differences ($p < 0.05$) compared to controls.

attachment surface 96-well round bottom plate (Corning Inc., Corning, NY). Following centrifugation, plates were maintained at 37 °C in a 5 % CO_2 incubator for 24 h to allow them to take on the usual 3-D spheroid form. 150 μl of supernatants from loaded Ma monolayers were added to the spheroid containing wells and the plates incubated for an additional 18 h. Light treatment at a radiant exposure of 2.4 and 4.8 J/cm^2 was used and spheroids were monitored for growth for an additional 14 days.

2.6. Hybrid Ma-F98 glioma spheroids

Hybrid tumor/Ma spheroids were formed as follows. Prior to spheroid formation, Ma^{PS} or Ma were incubated for 1 h in 20 μg ml^{-1} mitomycin C (Sigma-Aldrich Corp., St. Louis, MO) in order to inhibit cell division and their subsequent contribution to spheroid growth. Twenty-four hours following mitomycin treatment, the medium was replaced with medium containing $AlPcS_{2a}$ (2 μg/ml) for 4 h. The Ma were washed 4 times and counted. To form hybrid spheroids, Ma^{PS} or "empty" Ma were mixed with tumor cells at ratios of tumor cells to Ma or Ma^{PS} ranging from 1:2 to 2:1. In all cases, 2.5 × 10^3 /well of F98 cells and a variable number of Ma were aliquoted into the wells of an ultra-low attachment surface 96-well round bottom plate in 200 μl total volume. The plates were centrifuged at 1000 g for 10 min. 18 h after spheroid generation, light treatment (λ = 670 nm) at an irradiance of 4.0 mW/cm^2 was administered for 10 or 20 min (2.4 and 4.8 J/cm^2). Control spheroid cultures received either no Ma, or Ma^{PS} and no illumination. The hybrid spheroids were monitored for growth for an additional 14 days.

2.7. Fluorescence labeling of hybrid spheroids

Ma (20 × 10^6/ml) were labeled with PKH26GLRed (Fluorescent Cell Linker Kit, Sigma, St. Louis, MO). The F98 cell nucleus was stained with Hoechst 33,342 (blue) according to the manufacture's protocol. The labeled hybrid spheroids were visualized using an inverted Zeiss laser-scanning microscope (LSM 410, Carl Zeiss, Jena, Germany). Images were pseudo-colored blue and red. and were obtained at a depth of 80–100 μm within the spheroid.

2.8. Statistical analysis

All data was analyzed and graphed using Microsoft Excel. The arithmetic mean and standard deviation were calculated in all cases. Statistical significance was determined using the Student's *t*-test. Two values were considered significant when their p-values were below 0.05.

3. Results

3.1. Loading, and release of PS from Ma^{PS}

Ma were labeled with $AlPcS_{2a}$ for 4 h, washed and plated out in imaging dishes. Fluorescence microscopy was carried out after 1, 4 and 24 h to evaluate the time release of PS. The results are shown in Fig. 2a-c. At one hour, the cells presented bright fluorescence (Fig. 2a). The fluorescence was clearly diminished after 4 h (Fig. 2b) and disappeared after 24 h (Fig. 2c).

To further investigate the kinetics of Ma-PS release, PDT experiments were done using the collected SN at time intervals of 0.25 to 48 h. Light treatment was done at a radiance level of 1.2Jcm^2. The viability of F98 cell monolayers following SN mediated PDT is shown in Fig. 2d. Although some PDT effect was seen using SN collected after 2 h this was not significant compared to controls ($p > 0.05$). Significant effects ($p < 0.05$) were demonstrated after using SN harvested after 4, 24 and 48 h indicating that most of the PS was now released to the supernatant.

Since Ma have the funtion of degrading a large number of agents, the influence of Ma on the PDT response to free PS was also examined. Mitomycin treated Ma were co-incubated with an equal number of F98 cells (2.5 K). Fig. 2e shows the results for increasing PS concentrations. Light treatment was performed at a radiance level of 1.2 J/cm^2. As seen in the figure, the presence of Ma did reduce the effects of PDT on cell growth compared to controls. but the differences, although just reaching significants at some PS concentrations, were not pronounced.

3.2. Free and Ma released $AlPcS_{2a}$-mediated PDT

In order to establish baseline data for the effects on F98 spheroids of

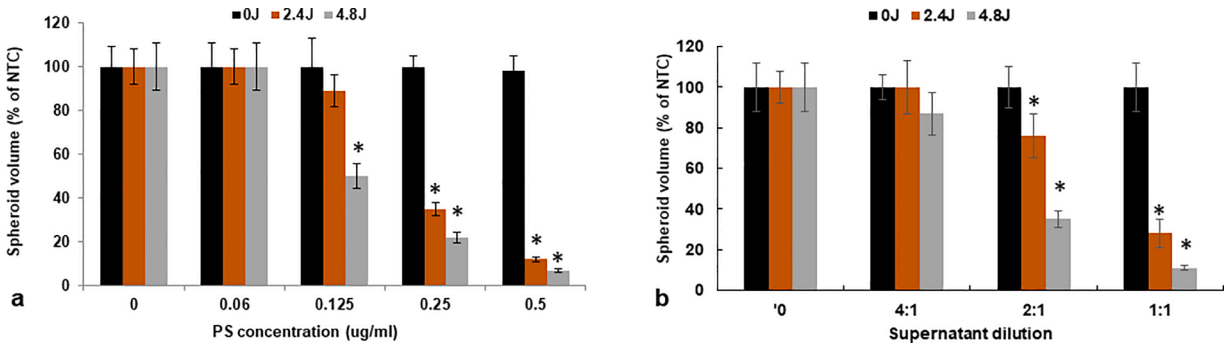

Fig. 3. Effect of PDT on the growth of F98 spheroids treated with free or Ma^{PS} released photosensitizer (PS). (a) PS concentration from 0 to 0.5 μg/mL. (b) PS containing supernatants harvested after 24 h. Radiance levels of 0, 2.4, and 4.8 J/cm^2. Each data point represents the average volume of 8 spheroids after 2 weeks in culture as a% of non-treated controls. Error bars, standard deviation. * significant differences ($p < 0.05$) compared to controls.

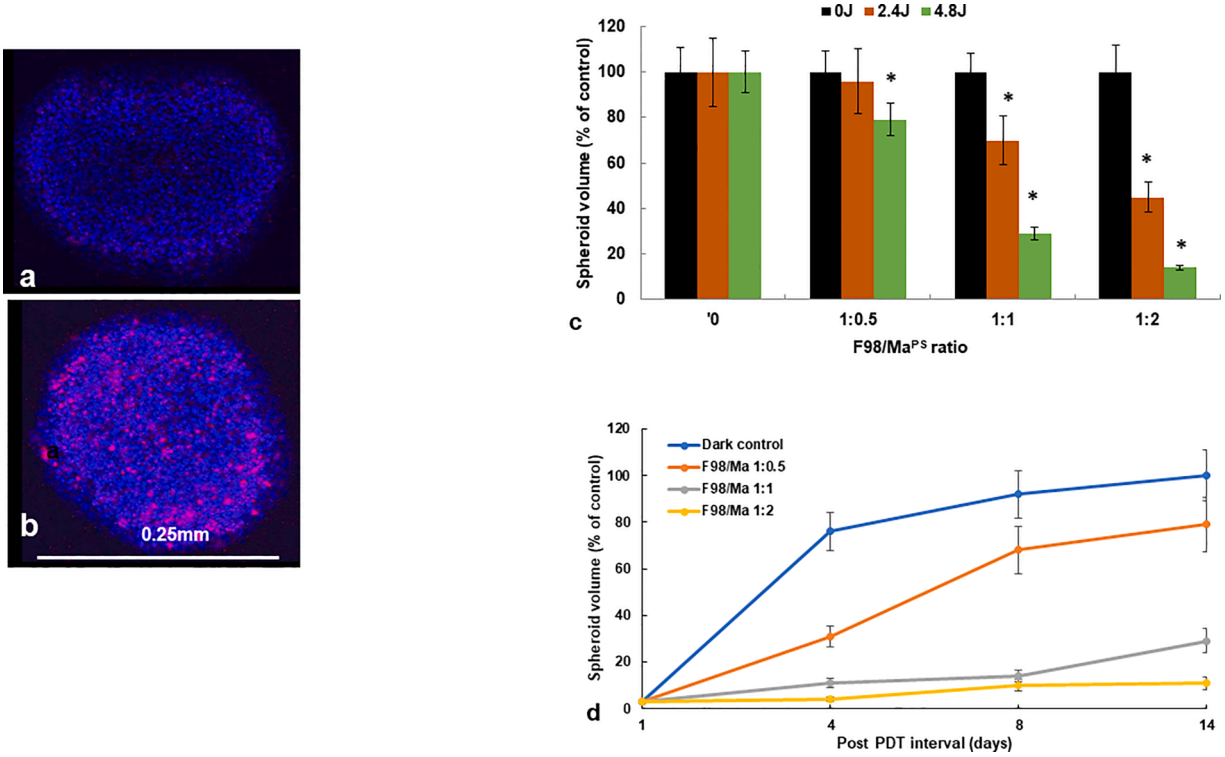

Fig. 4. Effect of PDT on the growth of F98/Ma^{PS} hybrid spheroids. Two photon fluorescence images (**a**) F98 spheroid. (**b**) F98/Ma^{PS} hybrid spheroid. Images taken 3 days after initiation. F98 Cell nucleus stained with Hoechst 33,342 (blue), Ma cytoplasm stained with PKH26 Red Fluorescent (red). Images were acquired at a depth of approximately 80–100 μm. **(c)** PDT on F98/Ma^{PS} hybrid spheroids ratio 1:0.5, 1:1, 1:2 PDT radiant levels 0, 2.4, 4.8 J/cm^2. (**d**) Growth kinetics of typical hybrid spheroids. Radiant exposure of 4.8 J/cm^2. Each data point represents the average volume of 16 spheroids from 2 experiments after 2 weeks in culture, as a% of non-treated controls. Error bars, standard deviation. * significant differences ($p < 0.05$) compared to controls.

$AlPcS_{2a}$ mediated PDT, experiments were first performed employing free photosensitizer. F98 spheroids, using 2.5 × 10^3 cells/well were aliquoted into the wells of round-bottom tissue culture microplates. Twenty-four hours later, PS was added to the wells at various concentrations ranging from 0 to 0.5 μg/ml and the incubation was continued for 24 h. Light treatment to a radiance of 2.4 and 4.8 J/cm^2 was administered at an irradiance of 4 mW/cm^2. The results are shown in Fig. 3a. Significant growth inhibition was seen at PS concentrations starting at 0.25 and 0.125 μg/ml for radiance levels of 2.4 and 4.8/cm^2, respectively (Fig. 3a). Not surprisingly, PDT-induced growth inhibition increased with increasing PS concentration. The results of these experiments therefore act as standard calibration data that can be compared to PDT effects utilizing Ma-released PS.

Similar spheroid experiments, as those described above for PDT-mediated free PS, were performed emloying supernatants containing released PS from loaded Ma, The Ma were pulsed with PS for 4 h, washed and supernatants containing released PS harvested after 24 h of incubation. The supernatants were diluted with medium at a ratio of 4:1 2:1 and 1:1. As shown in Fig. 3b, the PS-containing supernantants, in the absence of light treatment, were not inhibitory for spheroid growth even at the highest 1:1 dilution (dark control). In contrast, spheroid growth inhibition was significantly enhanced by PDT, at both radiance levels tested. Comparing the data shown in Fig. 3a to that shown in 3b, it was estimated that the Ma released PS at a 1:1 dilution corresponded to approximatly 0.3 μg/ml PS concentration.

3.3. PDT effect on hybrid Ma-F98 spheroid growth

Hybrid F98/Ma spheroids were formed as described in the materials and methods section.

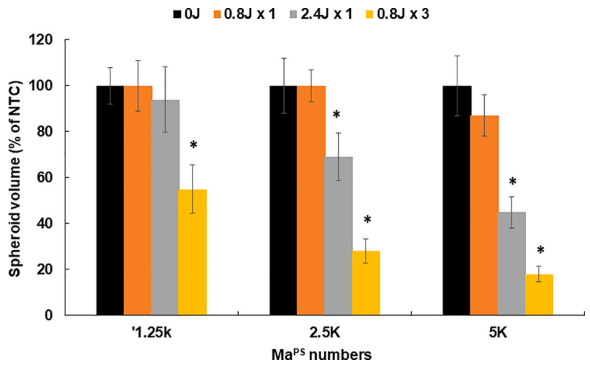

Fig. 5. Repetitive PDT of F98/Ma^{PS} hybrid spheroids. Hybrid spheroids, 2.5 K F98 and either 1.25, 2.5 or 5 K Ma^{PS}. Light treatment 0.8 J/cm^2 x 1, 2.4 J/cm^2 x 1 or 0.8 J/cm^2 x 3. Repetitive PDT; additional Ma^{PS} added on day 3 and 5. Light treatment, days 2, 4 and 6. Each data point represents the average volume of 18 spheroids from 3 experiments after 2 weeks in culture, as a% of non-treated controls. Error bars, standard deviation. * significant differences ($p < 0.05$) compared to controls.

The number of F98 cells to initiate the cultures was held constant at 2.5×10^3 and the number of Ma^{PS} ranged from 1.25×10^3 2.5×10^3 and 5×10^3 resulting in F98/Ma^{PS} ratios of 1:0.5, 1:1 and 1:2 respectively. Control hybrids containing empty Ma (no PS preincubation) were also included. Since the Ma were treated with the mitosis inhibiting agent Mitomycin, they did not contribute to spheroid growth. Light treatment was performed 24 h after spheroid initiation at radiant exposures of 2.4 and 4.8 J/cm^2. Two-photon fluorescence micrographs of a spheroid consisting of F98 cells and a hybrid spheroid of F98 and RAW264.7 at an initial ratio of 1:1 are shown in Figs. 4a and b, respectively. As seen in Fig. 4b, the Ma (red) were evenly distributed among the F98 cells (blue). The results of PDT on the growth of F98/Ma^{PS} hybrid spheroids after 14 days of incubation are shown in Fig. 4c. A significant decrease in spheroid growth with increasing radiance was observed at both radiance levels tested at F98/Ma^{PS} ratios of 1:1 and 1:2.

A substantial increase in PDT efficacy was observed by increasing the number of Ma^{PS} (5×10^3) especially at the highest radiant exposure investigated. Under these conditions, PDT resulted in spheroid sizes of 14 % of control volume, compared to 80% for a 2:1 F98/Ma ratio. The kinetics of typical spheroid growth over the 14-day incubation interval is shown in Fig 4d. Light treatment at a radiant exposure of 4.8 J/cm^2 was used. Dark controls reached control volumes (F98 spheroids) for all F98/Ma^{PS} cell ratios tested. F98/Ma^{PS} of 1:0.5 and 1:1 resulted in a growth delay but by day 14 the spheroids reached 29 % and 80 % of control values respectively. These spheroids were in a clear growth phase and would probably reach control values with time. In contrast, at 1:2 F98/Ma^{PS} ratio, spheroid growth was significantly inhibited at all time points.

3.4. *Repetitive Ma^{PS} -PDT*

Hybrid spheroids were formed on day 1 consisting of 2.5 k F98 and a variable number of Ma^{PS} 1.25, 2.5 and 5 k, respectively. Additional Ma^{PS} in amounts equal to those used on day 1, were added to the wells on day 3 and 5. Light treatment of 0.8 J/cm^2, or 2.4Jcm^2 were given as single treatment while repetitive light treatment of 0.8 J/cm^2 was administered in 3 equal doses 24 h after initial formation and after each Ma^{PS} addition. The results of an average of 3 experiments are shown in Fig. 5. A single radiant exposure of 0.8 J/cm^2 proved ineffective while a single exposure of 2.4 J/cm^2 produced significant growth inhibition. As shown in Fig. 5, 0.8 J /cm^2 administered 3 times was the most effective light delivery scheme investigated.

4. Discussion

The primary objective of this study was to examine the ability of Ma to act as vehicles for the delivery of sufficient concentrations of PS to glioma tumor cells for efficient PDT. It was hypothesized that: (1) Ma are capable of effective uptake and release of PS, (2) the PS is released mostly in a non-degraded form, and (3) PDT at $\lambda = 670$ nm irradiation results in growth inhibition of hybrid spheroids consisting of F98 glioma cells and PS-loaded Ma. The ability of Ma to take up and release PS is presented in Fig. 2. Specifically, the fluorescence images (Fig 2a-c) show that, following uptake, significant PS is released to the medium after a short time period (4 h) and, over a time course of approximately 24 h, all PS has been released.

An alternative interpretation of these results is that the Ma degraded the PS to the point that they were no longer capable of efficient fluorescence. Since significant PDT efficacy was observed using supernatant harvested after 4 h and at relatively low radiant exposures both on monolayers (Fig 2d) and F98 spheroids (Fig 3b), the results rule out significant PS degradation by Ma.That active PS was released from Ma is also corroborated by comparing the data shown in Fig. 3a and b. PDT mediated by either free or released PS showed no significant differences.

The results shown in Fig. 2e also indicate that Ma did not degrade PS to a large extent. The presence of empty Ma did reduce the effects of PDT on cell growth compared to controls but the differences, although just reaching significants at some PS concentrations, were not pronounced.

Compared to tumor cells, Ma have previously been shown to have a greater capacity to take up systemically administered PS [19,20]. Additionally, the multi-drug resistant protein P-gp, which actively pumps drug molecules out of cells, is highly expressed in the RAW264.7 Ma cell line used in the present study. These two characteristics likely account for the relatively high uptake and rapid export of PS from Ma which makes them suitable as transport vectors.

During tumor recurrence, usually in the vicinity of the surgical resection cavity, monocytes and macrophages are recruited into the tumor site by chemotaxis to enable new tumor growth.

Recent publications have also demonstrated that inflammation associated with surgical resection increases Ma migration to the resection site [21,22]. In addition, PDT in the brain has been shown to open the BBB resulting in increased Ma infiltration into the treated area [23,24].

The basic assumption for the use of Ma^{PS} as delivery vehicles, is that they function as PS release centers throughout the tumor cell infiltrated brain parenchyma and that the released PS will be taken up by the tumor cell population (Fig 1). The number of Ma^{PS} in proportion to the number of tumor cells is therefore a critical factor. The hybrid spheroids shown in Fig. 4 were designed as an *in vitro* simulation of a post-operative *in vivo* situation. The two-photon fluorescence image presented in Fig. 4b shows that the Ma were fairly evenly distributed throughout the spheroid. Significant PDT-induced growth inhibition was observed in hybrid spheroids (Fig. 4c), especially at lower F98/ Ma^{PS} ratios (1:2). Nevertheless, both at 2:1 and 1:1 F98/ Ma^{PS} ratios, spheroids were still in a growth phase and would eventually have reached control values if monitored for a sufficiently long time interval. These suboptimal ratios resulted in growth delays but did not lead to growth cessation, as demonstrated in Fig 4d. Proliferating cells in spheroids are found in the outer oxygen rich layers where spheroid growth takes place. Since PDT is oxygen dependent, it has its greatest efficacy on these proliferating cell layers. Cells located more centrally, in an oxygen poor environment, are more PDT resistant but can be recruited back into the proliferating population as the cells in the outer layers are killed [25]. The spheroids, after a delay, would therefore renew their growth. To overcome the inadequacies of single treatment, repetitive treatment protocols have been developed and have proven more effective [26,27]. This was confirmed in the present study where repetitive PDT (x3) with both low radiant exposures and repeat Ma^{PS} addition (Fig. 5) were found to be more effective than single treatment in this *in vitro* hybrid model. This is

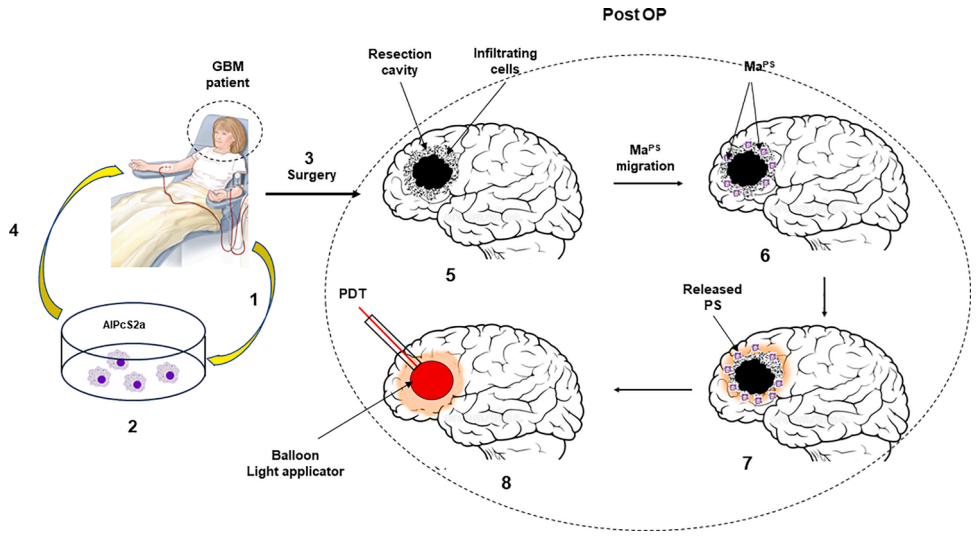

Fig. 6. Translation to proposed clinical protocol. (1) Ma extracted from the patient via leukapheresis. (2) Ma are *ex vivo* incubated with PS. (3) Tumor resection. (4) Ma^{PS} infused back into the patient. Post op. (5) resection cavity with remaining glioma cells. (6) Ma^{PS} infiltrate the resection cavity wall (7) release of PS. (8) light treatment (PDT) via a temporarily indwelling balloon applicator. Steps 4 and 8 repeated during week one of post op treatment.

an important point since translation to animal or clinical protocols is likely to require repetitive treatment. Repetitive PDT therefore has the dual advantage that it is more effective than single treatment and that PDT also significantly enhances the recruitment of Ma to the treatment site [23].

From a clinical perspective, repetitive PDT can be accomplished with the insertion of a balloon applicator into the resection cavity, facilitating light delivery over extended time periods [28]. Indwelling balloon applicators for light and radiation delivery have been implanted in patients during surgery and left in the resection cavity for up to one week before deflation and removal [29,30]. Conventional radiation and chemotherapy are typically delayed several weeks in order to allow for wound healing. During this delay, it is highly probable that disease progression occurs. Therefore, the type of approach, outlined above, allows for combined PDT and after-loading brachytherapy to be initiated post operatively shortly following tumor resection.

Targeting brain tumors with "precision," requires treatment protocols to be personalized [31]. An example of a personalized clinical protocol, involving the use of patient Ma as delivery vectors and a balloon applicator for light delivery, is illustrated in Fig. 6. Ma are extracted from the patient via leukapheresis. The Ma are cultured *in vitro*, incubated with PS and then infused back into the patient. The Ma^{PS} infiltrate the resection cavity wall and release the PS followed by repetitive PDT via an indwelling balloon applicator.

5. Conclusion

The results of the present study show a non-degraded release of $AlPcS_{2a}$ from loaded Ma, inducing effective PDT equivalent to that observed with free photosensitizer. The inhibition of $F98/Ma^{PS}$ hybrid spheroid growth, caused by Ma released PS-mediated PDT, was significantly enhanced by repetitive treatment. The results obtained in this study can be applied to further studies *in vivo,* which will require the development of a suitable post-op resection cavity animal model.

Ethical approval

This article does not contain any studies with human participants or animals, performed by any of the authors.

CRediT authorship contribution statement

Catherine Christie: Writing – original draft, Writing – review & editing, Visualization, Validation, Formal analysis. **Steen J Madsen:** Writing – review & editing, Validation, Formal analysis. **Qian Peng:** Formal analysis, Resources, Funding acquisition. **Henry Hirschberg:** Conceptualization, Methodology, Validation, Formal analysis, Resources, Data curation, Writing – original draft, Writing – review & editing, Visualization, Supervision, Project administration, Funding acquisition.

Declaration of Competing Interest

Conflict of Interest: All of the authors declare that she/he has no conflict of interest

Acknowledgments

The authors are grateful for the support from the Norwegian Radium Hospital Research Grant nr SE 1305

References

[1] M.C. Chamberlain, Radiographic patterns of relapse in glioblastoma, J. Neurooncol. 101 (2011) 319–323.
[2] M.C. Dobelbower, O.L. Burnett III, R.A. Nordal, L.B. Nabors, J.M. Markert, M. D. Hyatt, J.B. Fiveash, Patterns of failure for glioblastoma multiforme following concurrent radiation and temozolomide, J. Med. Imaging Radiat. Oncol. 55 (2011) 77–81.
[3] K. Petrecca, M.C. Guiot, V. Panet-Raymond, et al., Failure pattern following complete resection plus radiotherapy and temozolomide is at the resection margin in patients with Glioblastoma, J. Neurooncol. 111 (2013) 19–23.
[4] D. Bartusik-Aebisher, A. Zołyniak, E. Barnaś, A. Machorowska-˙Pieni ˛azek, P. Oleś, A. Kawczyk-Krupka, D. Aebisher, The use of photodynamic therapy in the treatment of brain tumors—a review of the literature, Molecules 27 (2022) 6847.
[5] D. Bhanja, H. Wilding, A. Baroz, M. Trifoi, et al., Photodynamic therapy for glioblastoma: illuminating the path toward clinical applicability, Cancers (Basel) 15 (2023) 3427.
[6] S.W. Cramer, C.C. Chen, Photodynamic therapy for the treatment of glioblastoma, Front Surg. 6 (2020) 81. Jan 21.
[7] B. Badie, J.M. Schartner, Flow cytometric characterization of tumor associated macrophages in experimental gliomas, Neurosurgery 46 (2000) 957–961, discussion 61-2.
[8] W. Roggendorf, S. Strupp, W. Paulus, Distribution and characterization of microglia/macrophages in human brain tumors, Acta Neuropathol. 92 (2004) 288–293, 1996.

[9] Carolina A., Fonseca C., and Badie B. Microglia, macrophages in malignant gliomas: recent discoveries and implications for promising therapies clinical and developmental immunology volume 2013.
[10] S. Valable, E.L. Barbier, M. Bernaudin, S. Roussel, C. Segebarth, E. Petit, et al., *In vivo* MRI tracking of exogenous monocytes/macrophages targeting brain tumors in a rat model of glioma, Neuroimage 40 (2) (2008) 973–983. Apr 1.
[11] M.R. Choi, K.J. Stanton-Maxey, J.K. Stanley, C.S. Levin, R. Bardhan, D. Akin, et al., A cellular Trojan horse for delivery of therapeutic nanoparticles into tumors, Nano Lett. 7 (12) (2007) 3759–3765.
[12] S.K. Baek, A.R. Makkouk, T. Krasieva, C.H. Sun, S.J. Madsen, H. Hirschberg, Photothermal treatment of glioma: an *in vitro* study macrophage-mediated delivery of gold nanoshells, J. Neurooncol. 104 (2) (2011) 439–448.
[13] S. Li, S. Feng, L. Ding, Y. Liu, Q. Zhu, Z. Qian, Y.1. Gu, Nanomedicine engulfed by macrophages for targeted tumor therapy, Int. J. Nanomed. 11 (2016) 4107–4124. Aug 23.
[14] C. Wang, K. Li, T. Li, et al., Monocyte-mediated chemotherapy drug delivery in glioblastoma, Nanomedicine (Lond) 13 (2018) 157–178.
[15] L. Pang, Y. Zhu, J. Qin, et al., Primary M1 macrophages as multi-functional carrier combined with PLGA nanoparticle delivering anti-cancer drug for efficient glioma therapy, Drug Deliv. 25 (2018) 1922–1931.
[16] D. Shin, C. Christie, D. Ju, R.K. Nair, S. Molina, K. Berg, T.B. Krasieva, S.J. Madsen, H. Hirschberg, Photochemical internalization enhanced macrophage delivered chemotherapy, Photodiagn. Photodyn. Ther. 21 (2018) 156–162.
[17] S.J. Madsen, H. Hirschberg, Macrophages as delivery vehicles for anticancer agents, Ther. Deliv. 10 (3) (2019) 189–201. Mar.
[18] A. Ivascu, M. Kubbies, Rapid generation of single-tumor spheroids for high-throughput cell function and toxicity, Anal. J. Biomol. Screen 11 (8) (2006) 922–932.
[19] M. Korbelik, G. Krosl, D.J. Chaplin, Photofrin uptake by murine macrophages, Cancer Res. (1991).
[20] M. Korbelik, M.R. Hamblin, The impact of macrophage-cancer cell interaction on the efficacy of photodynamic therapy, Photochem. Photobiol. Sci. 14 (8) (2015) 1403–1409. August.
[21] L. Hamard, D. Ratel, L. Selek, et al., The brain tissue response to surgical injury and its possible contribution to glioma recurrence, J. Neurooncol. 128 (2016) 1–8.
[22] H. Zhu, L. Leiss, N. Yang, et al., Surgical debulking promotes recruitment of macrophages and triggers glioblastoma phagocytosis in combination with CD47 blocking immunotherapy, Oncotarget 8 (No. 7) (2017) 12145–12157.
[23] H. Hirschberg, F.A. Uzal, D. Chighvinadze, M.J. Zhang, Q. Peng, S.J. Madsen, Disruption of the blood-brain barrier following ALA-mediated photodynamic therapy, Lasers Surg. Med. 40 (2008) 535–542.
[24] S.J. Madsen, H.M. Gach, S.J. Hong, F.A. Uzal, Q. Peng, H. Hirschberg, Increased nanoparticle-loaded exogenous macrophage migration into the brain following PDT-induced blood-brain barrier disruption, Lasers Surg. Med. 45 (8) (2013) 524–532.
[25] P.L. Olive, R.E. Durand, Drug and radiation resistance in spheroids: cell contact and kinetics, Cancer Metastasis Rev. 13 (1994) 121–138.
[26] S.J. Madsen, C.H. Sun, B.J. Tromberg, H. Hirschberg, Repetitive 5-aminolevulinic acid-mediated photodynamic therapy on human glioma spheroids, J. Neurooncol. 62 (3) (2003) 243–250. May.
[27] C.E. Olsen, A. Weyergang, V.T. Edwards, K. Berg, A. Brech, S. Weisheit, A. Høgset, P.K. Selbo, Development of resistance to photodynamic therapy (PDT) in human breast cancer cells is photosensitizer-dependent: possible mechanisms and approaches for overcoming PDT-resistance, Biochem. Pharmacol. 144 (2017) 63–77. Nov 15.
[28] S.J. Madsen, C.H. Sun, B. Tromberg, H. Hirschberg, Development of a novel balloon applicator for optimizing light delivery in photodynamic therapy, Lasers Surg. Med. 29 (2001) 406–412.
[29] T.B. Johannesen, K. Watne, K. Lote, J. Norum, J.R. Henning, K. Tvera, H. Hirschberg, Intracavity fractionated balloon brachytherapy in glioblastoma, Acta Neurchiurica 141 (2) (1999) 127–133.
[30] M.S. Eljamel, C. Goodman, H. Moseley, ALA and Photofrin fluorescence-guided resection and repetitive PDT in glioblastoma multiforme: a single center phase III randomized controlled trial, Lasers Med. Sci. 23 (2008) 361–367.
[31] A.M. Tsimberidou, E. Fountzilas, M. Nikanjam, R. Kurzrock, Review of precision cancer medicine: evolution of the treatment paradigm, Cancer Treat. Rev. 86 (2020), 102019. Jun.